

Electronic Supporting Information

In-situ developed $\text{NiCo}_2\text{O}_4\text{-Ti}_3\text{C}_2\text{T}_x$ nanohybrid towards non-enzymatic electrochemical detection of glucose and hydrogen peroxide

Devarasu Mohanapriya and Kathavarayan Thenmozhi*

Department of Chemistry, School of Advanced Sciences, Vellore Institute of Technology (VIT), Vellore-632014, India.

Email: *Kathavarayan Thenmozhi: k.thenmozhi@vit.ac.in; kt.thenmozhi@gmail.com

Materials and methods

MAX phase with approximately 40 mesh size were purchased from Nano Research Element, India. Lithium fluoride (LiF), ascorbic acid (AA) and hydrogen peroxide (H_2O_2) dopamine hydrochloride (DA) were purchased from Sigma Aldrich, India. Cobalt (II) chloride hexahydrate, nickel (II) chloride hexahydrate, uric acid (UA), cholesterol (Chol), glucose (Glu), tryptophan (L-Tryp), potassium chloride (KCl) and cystine (Cys) were obtained from SRL chemicals, India. Potassium perchlorate (KClO_3) was produced from Alfa Aesar, India. Leucine (Leu) was obtained from Sd Fine Chemicals, India and potassium nitrite (KNO_3) was purchased from Avra Chemicals, India. Valine (Val) was bought from Spectrochem, India. All of the acquired compounds were of AR grade and were utilized without additional purification. All sample solutions were prepared using Milli-Q water.

Instrumentation

Bruker D8 advance instrument was used to record the powder X-ray diffraction (PXRD) pattern of the synthesized nanohybrid. Thermo-Fisher FEI QUANTA 250 FEG was used to carry out the Field Emission Scanning Electron Microscopic (FE-SEM) analysis. High-resolution transmission electron microscopic (HRTEM) images were obtained on JEOL JEM 2100 with a LaB6 electron source. PHI5000 Version Probe III was employed to examine the X-ray photoelectron spectroscopic (XPS) information. The CHI-760E electrochemical workstation was utilised for all the electrochemical investigations. A standard three-electrode setup was employed, consisting of a platinum coil functioning as the counter electrode, Ag/AgCl as the reference electrode and glassy carbon as the working electrode.

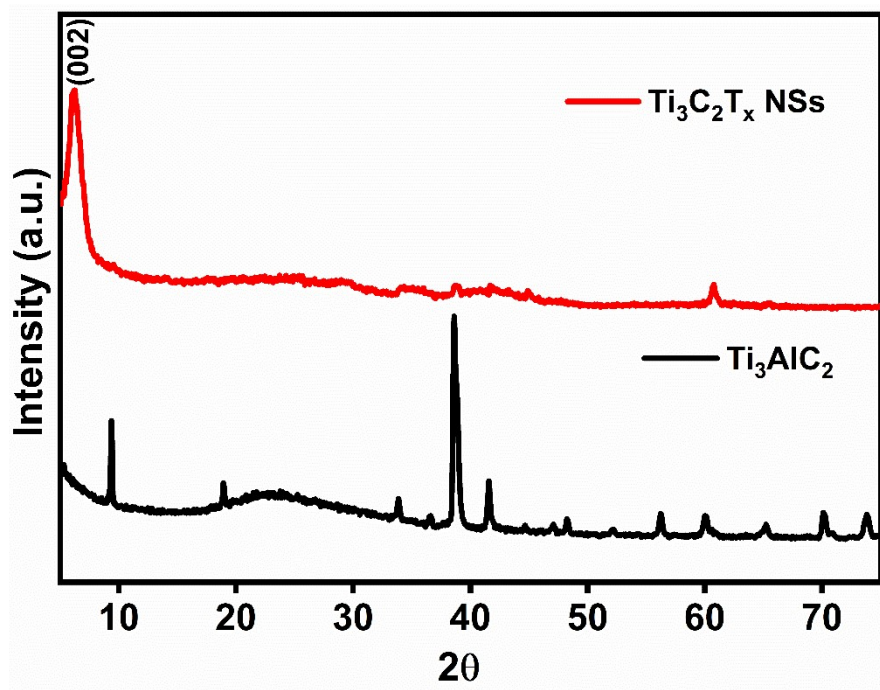


Figure S1. XRD patterns of Ti_3AlC_2 (black) and $\text{Ti}_3\text{C}_2\text{T}_x$ MXene (red).

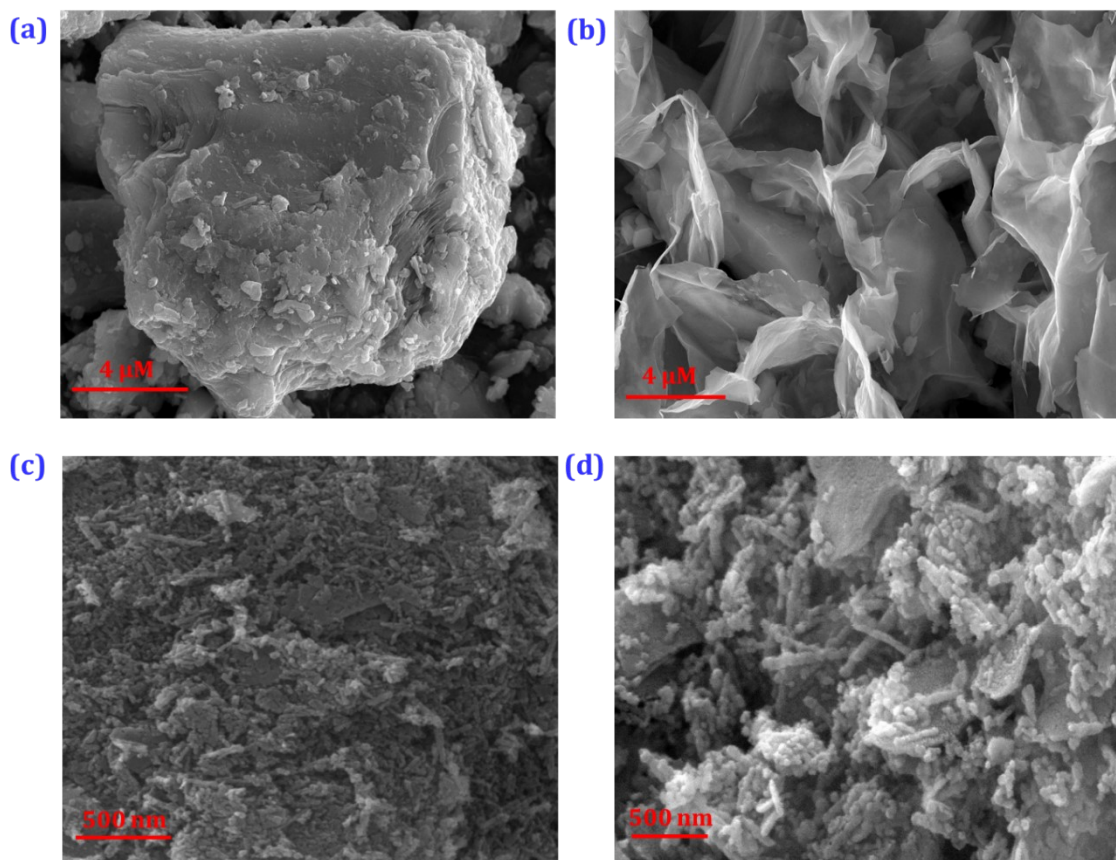


Figure S2. FESEM images of (a) Ti_3AlC_2 (b) $\text{Ti}_3\text{C}_2\text{T}_x$ NSs (c) NiCo_2O_4 NPs and (d) NiCo_2O_4 - $\text{Ti}_3\text{C}_2\text{T}_x$ nanohybrid.

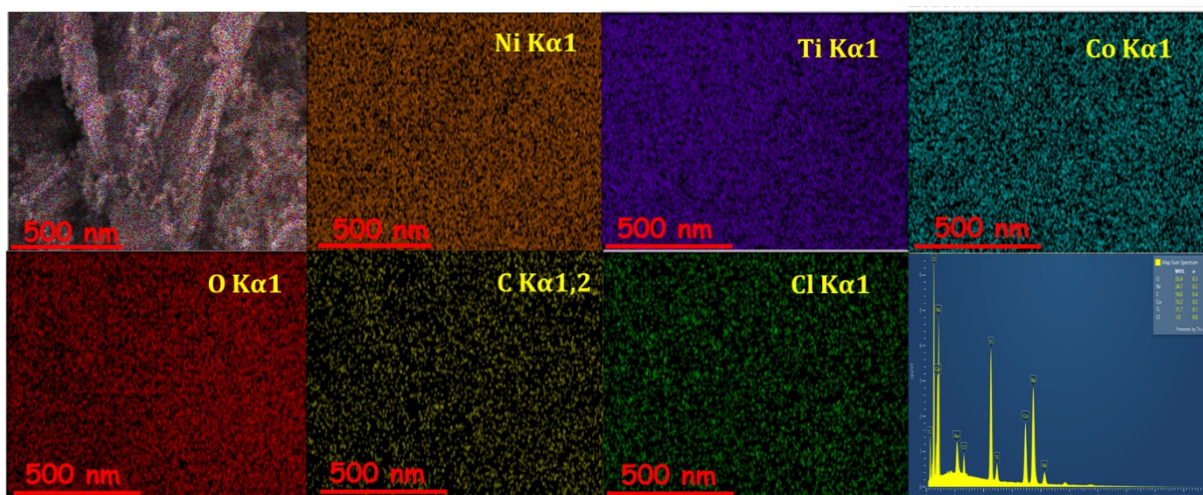


Figure S3. FESEM image and elemental analysis of the $\text{NiCo}_2\text{O}_4\text{-Ti}_3\text{C}_2\text{T}_x$ nanohybrid.

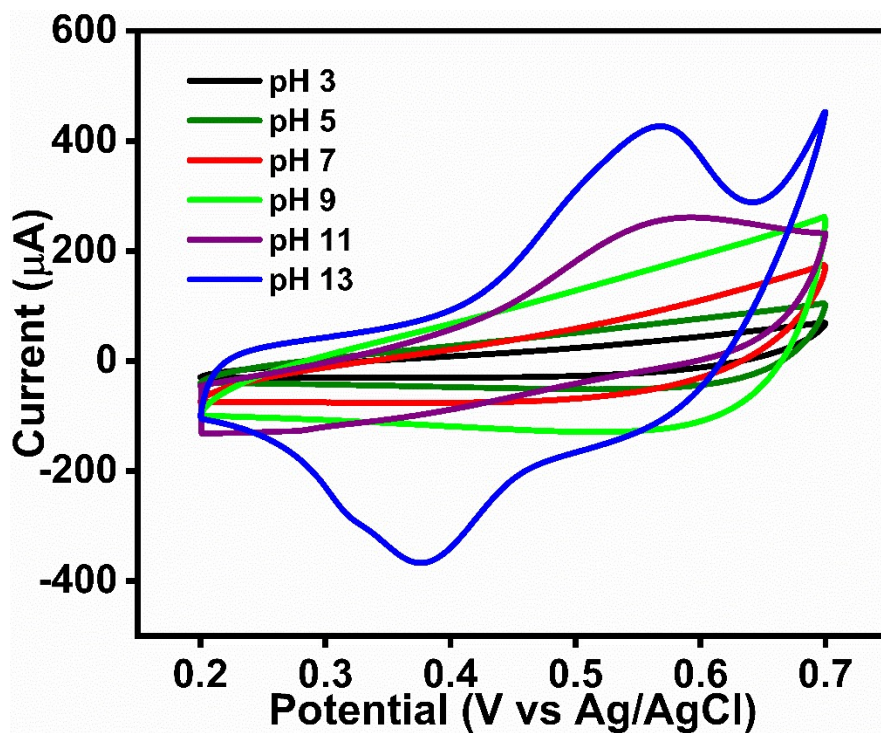


Figure S4. Effect of pH on the electrochemical behaviour of $\text{NiCo}_2\text{O}_4\text{-Ti}_3\text{C}_2\text{T}_x/\text{GCE}$.

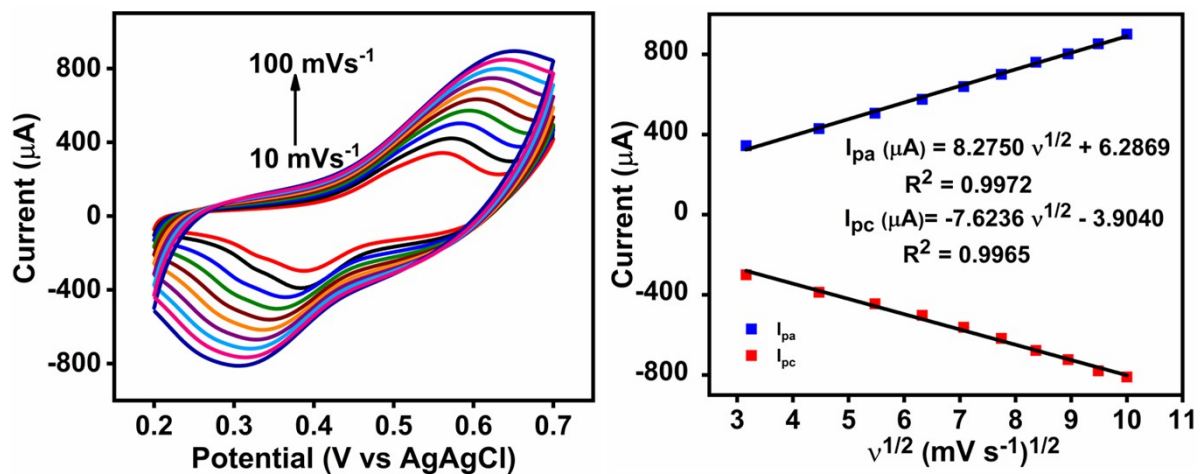


Figure S5. (a) Effect of scan rate and (b) corresponding calibration plot.

Table S1. Real time detection of Glu in serum and urine samples.

Sample	Spiked	Found^a	Recovery (%)
Serum	100 mM	97.6 mM	97.6
	200 mM	203.1 mM	101.5
Urine	100 mM	98.2 mM	98.2
	200 mM	201.6 mM	100.8

Sample	Spiked	Found^a	Recovery (%)
Milk	50 mM	48.9 mM	97.8
	100 mM	102.1 mM	102.1
Apple Juice	50 mM	47.8 mM	95.6
	100 mM	105.6 mM	105.6

Table S2. Real time detection of H₂O₂ in milk and apple juice samples.

Electrode material	Analyte	Operating potential (V)	Linear range (μM)	LOD (μM)	Sensitivity	Ref.
MXene/CoNiMn/GCE	Glu	0.5	10 - 900	0.24	-	1
MXene-Cu ₂ O/GCE	Glu	0.6	0.01 - 3000	2.4	11.061 $\mu\text{A mM}^{-1} \text{cm}^{-2}$	2
Co ₃ O ₄ /MXene@CFE	Glu	0.55	0.05 - 7440	0.01	19.3 $\mu\text{A mM}^{-1} \text{cm}^{-2}$	3
Nickel-copper oxide NPs@ 3D-rGO/MWCNT/GCE	Glu	0.6	0.1 - 900	0.04	-	4
NiCo ₂ O ₄ /RDE	H ₂ O ₂	-0.58	0 - 14000	0.05	392.5 $\text{mA mM}^{-1} \text{cm}^{-2}$	5
MX/CS/PB/GCE	H ₂ O ₂	0.0	0.05 - 667	0.004	-	6
Cu _x O/Ag@FLG/GCE	H ₂ O ₂	-0.65	10 - 100000	2.13	174.5 $\mu\text{A mM}^{-1} \text{cm}^{-2}$	7
Co ₃ O ₄ /ATNTs	H ₂ O ₂	-0.6	1.27 - 26.80	6.71	39.53 $\mu\text{A mM}^{-1} \text{cm}^{-2}$	8
NiCo ₂ O ₄ -Ti ₃ C ₂ T _x MXene-GCE	Glu	0.5	30 - 1830	9	101.2 $\mu\text{A } \mu\text{M}^{-1} \text{cm}^{-2}$	This work
	H ₂ O ₂	-0.25	20 - 100 100 -2010	6	107.03 $\mu\text{A } \mu\text{M}^{-1} \text{cm}^{-2}$	This work

Table S3. Comparative performances of NiCo₂O₄-Ti₃C₂T_x/GCE sensor with recently reported Glu and H₂O₂ sensors.

References

- 1 K. Kasirajan, P. Rajkumar, H. G. Kwon, J. H. Yim, J. Kim and H. K. Choi, *Appl Mater Today*, 2024,39, 102263.
- 2 T. S. Gopal, S. K. Jeong, T. A. Alrebdi, S. Pandiaraj, A. Alodhayb, M. Muthuramamoorthy and Andrews Nirmala Grace, *Mater Today Chem*, 2022, 24, 100891.
- 3 D. Manoj, A. Aziz, N. Muhammad, Z. Wang, F. Xiao, M. Asif and Y. Sun, *J Environ Chem Eng*, 2022, 10, 108433.
- 4 Z. Taji, A. A. Ensafi, E. Heydari-Soureshjani and B. Rezaei, *Electroanalysis*, 2021, **33**, 304–313.
- 5 J. Jiang, Z. Zhang, C. Yang, R. Wang and Z. Wu, *RSC Adv*, 2022, **12**, 35199–35205.
- 6 F. Zhu, X. Wang, X. Yang, C. Zhao, Y. Zhang, S. Qu, S. Wu and W. Ji, *Analytical Methods*, 2021, **13**, 2512–2518.
- 7 J. Song, Y. Wan, C. Yang, Q. Deng, Y. Cui, Z. Yan and Y. Liu, *Sci Rep*, 2023, 13, 6640.
- 8 R. Ullah, M. A. Rasheed, S. Abbas, K. ul Rehman, A. Shah, K. Ullah, Y. Khan, M. Bibi, M. Ahmad and G. Ali, *Current Applied Physics*, 2022, **38**, 40–48.